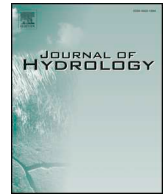




ELSEVIER

Contents lists available at ScienceDirect

Journal of Hydrology

journal homepage: www.elsevier.com/locate/jhydrol

Research papers

Intra-specific variability in deep water extraction between trees growing on a Mediterranean karst

Simon Damien Carrière^{a,*}, Julien Ruffault^b, Coffi Belmys Cakpo^c, Albert Olioso^d, Claude Doussan^d, Guillaume Simioni^b, Konstantinos Chalikakis^e, Nicolas Patris^f, Hendrik Davi^b, Nicolas K. MartinSt-Paul^b

^a Sorbonne Université, UPMC, CNRS, EPHE, UMR 7619 METIS, 4 place Jussieu, 75005 Paris, France

^b INRAE, URFM, Domaine Saint Paul, INRAE Centre de recherche PACA, 228 route de l'Aérodrome, CS 40509, Domaine Saint-Paul, Site Agroparc, France

^c INRAE, PSH, Domaine Saint Paul, INRAE Centre de recherche PACA, 228 route de l'Aérodrome, CS 40509, Domaine Saint-Paul, Site Agroparc, France

^d INRAE, UMR 1114 EMMAH, Domaine Saint Paul, INRAE Centre de recherche PACA, 228 route de l'Aérodrome, CS 40509, Domaine Saint-Paul, Site Agroparc, France

^e Avignon Université, UMR 1114 EMMAH, 301 rue Baruch de Spinoza, BP 21239 84911 Avignon Cedex 9, France

^f IRD, Hydrosience Montpellier, 300 Avenue du Professeur Emile Jeanbrau, 34090 Montpellier, France

ARTICLE INFO

This manuscript was handled by Corrado Corradini, Editor-in-Chief, with the assistance of Junbing Pu, Associate Editor

Keywords:

Drought tolerance
Quercus ilex
 Isotopy
 Hydrogeophysics
 Leaf water potential
 Intra-specific
 Mediterranean karst

ABSTRACT

Plant transpiration is a major component of water fluxes in the critical zone, which needs to be better characterized to improve our ability to understand and model the hydrological cycle. In water-limited ecosystems such as those encountered on karst environments, climate-induced changes in transpiration are expected to be strongly influenced by the ability of the vegetation cover to resist or adapt to drought. However, because of the high heterogeneity of karst environments, the amount of water available for trees can change within a stand, which may lead to significant differences in drought vulnerability resistance between trees of the same species. So far it is not known if soil and subsoil environment influence the magnitude of deep water extraction, at the intra-specific scale. Here, we investigate the variability in deep water extraction for six individual *Quercus ilex* trees growing on a karst substrate in a Mediterranean forest. We combined three approaches: (i) electrical resistivity tomography to determine the variability of soil/subsoil characteristics, (ii) isotope tracing to determine the origin of water transpired by plants, and (iii) predawn and midday leaf water potential (Ψ) to assess the trees' water stress and transpiration regulation. Along the summer season, deep water extraction increased with drought intensity. Deep water use varies between individuals and according to drought intensity. At moderate water stress levels, we found no significant relationship between the origin of xylem water and soil/subsoil characteristics or individual stress level. However, at the peak of the drought (average predawn $\Psi < -2$ MPa), individuals that had the least total available water in soil/subsoil (0–2 m) relied more on deep water and were also subject to less water stress. These results suggest that trees with less favorable soil/subsoil conditions (i.e. low water retention capacity) in the near surface (0–2 m) adapt their root systems to exploit deep water reserves more intensively so as to enhance their drought tolerance, while trees with more favorable surface conditions exhibit greater water stress and may be more vulnerable to extreme droughts because of a lower root development in deeper horizons.

1. Introduction

On one side, a large part of continental precipitation is transpired at the world scale (e.g. Oki and Kanae, 2006; Maréchal et al., 2009; Fisher et al., 2017). On the other side, the water availability is one of the most important factors driving transpiration, biomass productivity, and plant species distribution in water-limited ecosystems (Rambal et al., 2003; Mathys et al., 2014). Understanding forest response to droughts is a crucial issue under climate change, because of their multiple impacts on

ecosystems and society (Kirilenko and Sedjo, 2007; Bonan, 2008; Taylor et al., 2013). Indeed, ongoing climate change has a strong impact on vegetation (Allen et al., 2010; Anderegg, 2015) and changes in vegetation cover have a strong impact on hydrological processes (Scanlon et al., 2005; Noretto et al., 2012). Deciphering the complex interactions between vegetation cover and hydrological processes is crucial to improve the predictability of climate changes impacts on the hydrological cycle.

The capacity to withdraw water in deep water is a key feature of

* Corresponding author.

<https://doi.org/10.1016/j.jhydrol.2020.125428>

drought tolerance (Ehleringer et Dawson, 1992; Querejeta et al., 2007; Pivovarov et al., 2016; Brum et al., 2019) that is known to vary among species and contributes, together with other traits, to define the hydrological niches (Brum et al., 2019).

Drought tolerance variability at the intra-specific level, and within a same population, is expected to have a key influence on the evolutionary potential of forests under climate change, and could thereby constitute an important source of resilience to drought (Bontemps et al., 2017). It could result from of adaptation or plasticity in response to micro local environmental variations.

However there are less data available at intra-specific level, and in particular, the role of deep water exploration for drought tolerance is less clear. Voltas et al. (2015) showed that genetic factors could explain differences in water use on Aleppo pines of various origins grown in common garden test. Barbeta et al. (2015) showed that plasticity could lead to differences in water exploitation for individuals located in a rain exclusion zone and those located in the control zone. Some studies have suggested that micro local variability in soil/subsoil conditions (i.e. water retention capacity, stoniness, soil depth) also explains intra-specific variations of both leaf and tree scale traits (e.g. leaf mass area, foliar $\delta^{13}\text{C}$, leaf area index, predawn leaf water potential), (Love et al., 2019; Preisler et al., 2019; Carrière et al., 2020a). More specifically, they suggest that trees with less favorable soil environments have greater acclimation to drought and experience lower water stress and dieback during extreme drought (than trees with higher total available water (TAW)) within soil. But this theory implies two related hypotheses that so far have not been rigorously tested: i) a relationship exists between near-surface soil/subsoil conditions and the ability of individuals to exploit deep water, and ii) this relationship may affect the resistance of individuals to drought.

In this study we aim to assess the relationship between tree water stress, soil/subsoil characteristics, and tree capacity to withdraw deep water, on 6 individual *Quercus ilex* stems. In particular we explore if soil/subsoil conditions consistently affect tree level water stress and trees' ability to draw water at several depths.

For these purposes, we chose to work in a karst settings where the soil/subsoil conditions are expected to be strongly contrasted between individuals due to the intrinsic heterogeneity of this media (Hartmann et al., 2014). In this type of environment, strong contrasts in soil thickness, stoniness and water retention capacity can induce a strong variability of soil/subsoil conditions in a few meters, which in turn might influence the develop of root systems for vegetation. We combine three distinct approaches: geophysical, isotopic, and eco-physiological. The first approach, Electrical Resistivity Tomography (ERT), is a non-destructive near-surface geophysical technique used to characterize variability in soil/subsoil conditions (Dahlin, 2001; Chalikhakis et al., 2011). Unlike classical techniques (e.g. pedologic pits, neutron probe, or Time Domain Reflectometry (TDR) sensors for water), ERT provides an integrated and spatialized (horizontally and vertically) characterization of the near surface at the plot scale. The second approach is water isotope tracing ($\delta^{18}\text{O}$), which is used to determine the source of water extracted by plants (Dawson, 1993; Querejeta et al., 2007; Nie et al., 2012; Ding et al., 2018). The third approach uses shoot water potential (Ψ), which is widely used to assess plant water stress (Turner, 1981). When measured at predawn, transpiration is close to zero, leaf water potential provides an estimate of soil water deficit in the rooting zone. However, when measured during daytime, water potential measurements results from both, soil water deficit and plant hydraulics and transpiration. All datasets used in this study have been described and investigated in previous papers. Carrière et al. (2020a) used ERT to study the variability of foliar traits in response to drought. Carrière et al. (2020b); c) used water isotope combined with predawn and midday leaf water potential to study the variability of deep water use among three species. In this paper, we combine geophysical, isotopic, predawn and midday leaf water potential dataset in an original way to explore the variability of deep water use between individuals of the

same species.

2. Material and methods

2.1. Experimental site

The experimental forest site is located in southern France within the Fontaine-de-Vaucluse observatory (43°56'12"N; 5°27'58"E; 530 m a.s.l.), which is part of the French critical zone observation network (OZCAR – <http://www.ozcar-ri.org/>; Jourde et al., 2018). The plot, which measures 150*50 m, is dominated by *Quercus ilex* L. (85% of the basal area) and an understory (15% of the basal area) dominated by shrubs including *Buxus sempervirens* L., *Juniperus communis* L. and *Juniperus phoenicea* L. (more details can be found in Carrière et al. (2017)). The forest was managed as a coppice for charcoal production for centuries before the last clear-cut 90 years ago.

The climate is Mediterranean with dry and hot summers; most rainfall occurs during spring and autumn. Between 2003 and 2015, average annual rainfall was 909 mm and ranged between 407 and 1405 mm. Average annual temperature over the same period was 12.9 °C. The soil is a stony rendzina whose thickness is highly variable over the study site. Soil pits excavated along the profile revealed soil depths ranging from 0 to 70 cm. This soil has developed on a karstified calcareous bedrock of Urgonian facies.

Under the experimental plot, a former military bunker has been converted into a scientific laboratory (<http://lsbb.eu/presentation/>). This underground facility provides an opportunity to sample water flows in the vadose zone at depths of 33 and 256 m. Surface-based geophysical exploration showed, with ERT, that the first two meters of the soil/subsoil can store considerable amounts of water (several tens of millimeters) but with high spatial variability at the plot scale (Carrière et al., 2015). Deeper (2–90 m) magnetic resonance sounding (MRS) and gravimetry showed seasonal relative variations in water storage that can reach 50% within the vadose zone (Carrière et al., 2016).

2.2. Electrical resistivity tomography

The ERT dataset used in this study was described by Carrière et al. (2015) and then re-used by Carrière et al. (2020a) to assess spatial variability of soil/subsoil conditions (i.e. TAW) at the plot level. Additional methodological details about ERT measurements can be found in those two studies. ERT measurements were done using an ABEM Terrameter SAS 4000 device (Dahlin, 2001) with 64 stainless steel electrodes and 2 m spacing along a 126 m transect. The measurement protocol that was used recorded 1140 points. The transect was chosen to align almost perpendicularly to the slope and geological structures (Carrière et al., 2013) to maximize the variability in soil/subsoil conditions. The inversion quality of the ERT data was evaluated with RMS and Chi^2 , calculated using the raw data and the inverted model (lower-left corner of each cross-section; Fig. 1). The resistivity model had a 2 m lateral resolution and a vertical resolution ranging gradually from 0.5 m near the surface to 1.5 m at the base of the cross-section (10 m). A temperature correction was applied on the final model, following Keller and Frischknecht (1966):

$$\rho = \rho_T [1 + \alpha(T - 25)] \quad (1)$$

where ρ (Ωm) is electrical resistivity at the reference temperature of 25 °C, ρ_T (Ωm) is electrical resistivity measured at temperature T (°C), and α is 0.0202. T is underground temperature, logarithmically interpolated between daily mean air temperature aboveground and groundwater temperature at a depth of 30 m.

The Percent Variation in Resistivity (PVR) was used to describe the spatial variability of soil/subsoil conditions under each *Quercus ilex* L. individual. PVR was calculated for each tree as a function of the dry (ρ_{dry}) and wet (ρ_{wet}) resistivity cross-section, as in Clément et al. (2010) and Robert et al. (2012):

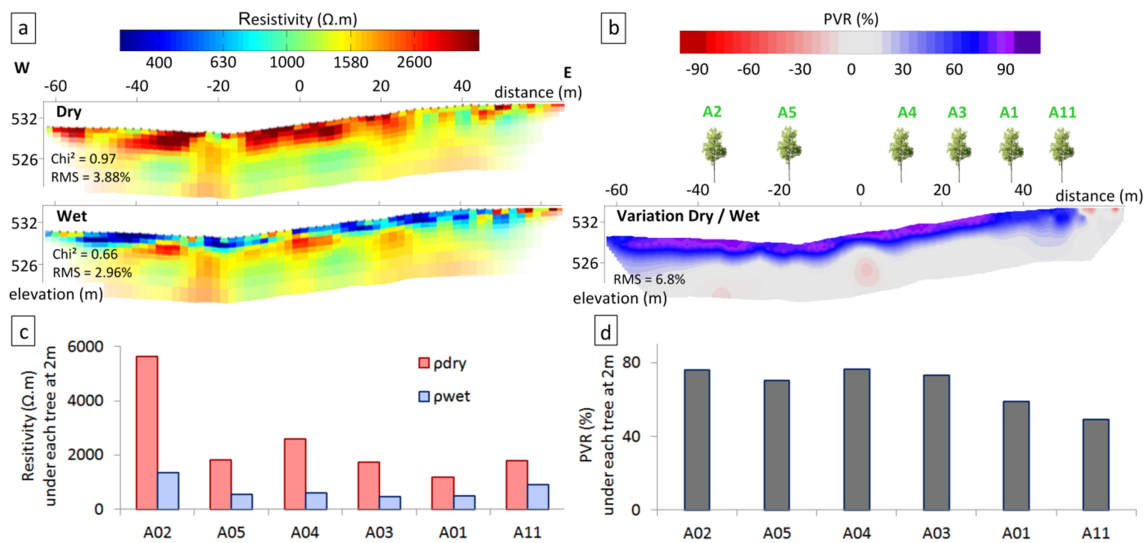


Fig. 1. Electrical Resistivity Tomography (ERT) results. (a) ERT models for the “dry” and “wet” dates (respectively before and after a rain event in November 2011), involved in PVR computation (Eq. (2)); Gradient arrays, 64 electrodes; ERT model uncertainty, based on current line density, is represented by the color attenuations at the edges and the bottom of the resistivity cross-section. (b) Percent variation in resistivity (PVR) between the two resistivity models (dry/wet). (c) Resistivity averaged over 2 m under each tree in dry (ρ_d) and wet period (ρ_w). (d) PVR averaged over 2 m under each tree.

$$PVR(\%) = \frac{\rho_{dry} - \rho_{wet}}{\rho_{dry}} * 100 \quad (2)$$

Two ERT measurements were successively carried out in autumn 2011 at an interval of a few days ranging from an extremely dry (i.e. 3 months of drought) to an extremely wet (i.e. after an episode of 230 mm rainfall) status (Fig. 1a). The temporal proximity of these measurements and similar meteorological conditions between these two days resulted in very limited variations in air and groundwater temperatures. In Carrière et al. (2020a), we showed that PVR between these two dates can be used as a proxy for the total available water (TAW) for vegetation (Fig. 1b). The near surface PVR was calculated for each individual by a lateral average within a distance of 2.5 m (corresponding to crown radius) to the stool center and vertically between 0 and 2 m. This thickness corresponds on average to the depth of the massive limestones previously detected by ground penetrating radar (Carrière et al., 2013). We consider that the TAW (0–2 m) of each tree is fix parameter in time for a 90 years old stand and that it is its degree of filling that varies over the seasons according to drought level. Therefore, the PVR, which is a proxy of TAW, was measured only once in 2011.

2.3. Isotopic tracing

2.3.1. Sampling

The isotopic dataset was published in Carrière et al. (2020c). Field work was conducted on 6 trees at monthly time step between June and August 2015 (06/11/2015; 07/06/2015; 08/11/2015). On each date, three to four sunny branches with a diameter of 4–6 mm were collected from each tree at midday. Phloem and bark were removed to prevent any contamination from phloem sap. The samples were immediately packed in parafilm and placed in sealed vials. These three to four branches were pooled before extraction. A portable cooler was used to transfer the samples to the laboratory where they were stored frozen until water extraction and analyses. Liquid samples of precipitation and drainage water were collected every 1 to 3 weeks. Precipitation was collected through a pluviometer and stored in containers installed in a pit so as to limit temperature variations. Drainage water was collected at 20 cm below the surface using a mini-lysimeter and this water was stored in a separate container (see Fig. in SI1). These containers were maintained at atmospheric pressure through a capillary to limit

exchange between the atmosphere and collected water (IAEA, 2014), (see Fig. SI1). The samples were collected on a monthly time step basis and were therefore a mixture of all the water flowed into the cans during the previous month. At this experimental site, the rocky karst soil prevents soil water sampling using auger drilling or porous cups.

2.3.2. Water extraction and isotopic analyses

Xylem water was extracted from wood by cryogenic vacuum distillation following the protocol of West et al. (2006). The twigs were cut into small pieces and placed in an electrothermal heating and stirring mantle at 90 to 100 °C for 1 h. Two successive liquid nitrogen traps were used to collect 3 to 5 ml of xylem water. This water was stored in small vials until analyzed.

Deep water and shallow water samples were analyzed using a Los Gatos Isotope Ratio Infrared Spectrometer (IRIS) at Avignon University (LGR DLT-100 liquid water stable analyzer accuracy $\pm 0.2\%$ vs V-SMOW for $\delta^{18}O$). The isotopic ratios were expressed as:

$$\delta^{18}O = [(R_{sample}/R_{standard}) - 1] \times 1000\% \quad (3)$$

where $R_{standard}$ and R_{sample} are the light/heavy isotope ratios ($^{16}O/^{18}O$) of the sample and the standard (Vienna Standard Mean Ocean Water (VSMOW)), respectively. Possible spectral perturbations of the IRIS measurements due to organic contaminants in xylem and drainage samples (Martín-Gómez et al., 2015) motivated us to use an Isotope Ratio Mass Spectrometer (IRMS). Xylem and drainage samples were analyzed using the Isoprime IRMS at the LAMA laboratory of Hydro-Sciences Montpellier, using the CO_2 equilibration technique in dual inlet mode, yielding $\delta^{18}O$ results with a $\pm 0.06\%$ precision. This value was obtained by calculating the standard deviation related to repeated measurements of a standard sample during the analysis of our samples. This precision is reported in Fig. 2b and c in the $\delta^{18}O$ error bars.

2.4. Leaf water potential

The predawn (Ψ_p) and midday (Ψ_m) leaf water potential dataset was previously published in Carrière et al. (2020a). Both metrics were measured on the 6 individuals chosen for isotope sampling throughout the 2015 summer season using a Scholander pressure bomb. Samples for Ψ_p were collected in the morning, before sunrise. For Ψ_m , samples were collected from sun-exposed branches around midday (2PM GMT), when the sky was not cloudy. For each tree, at least four leaves were

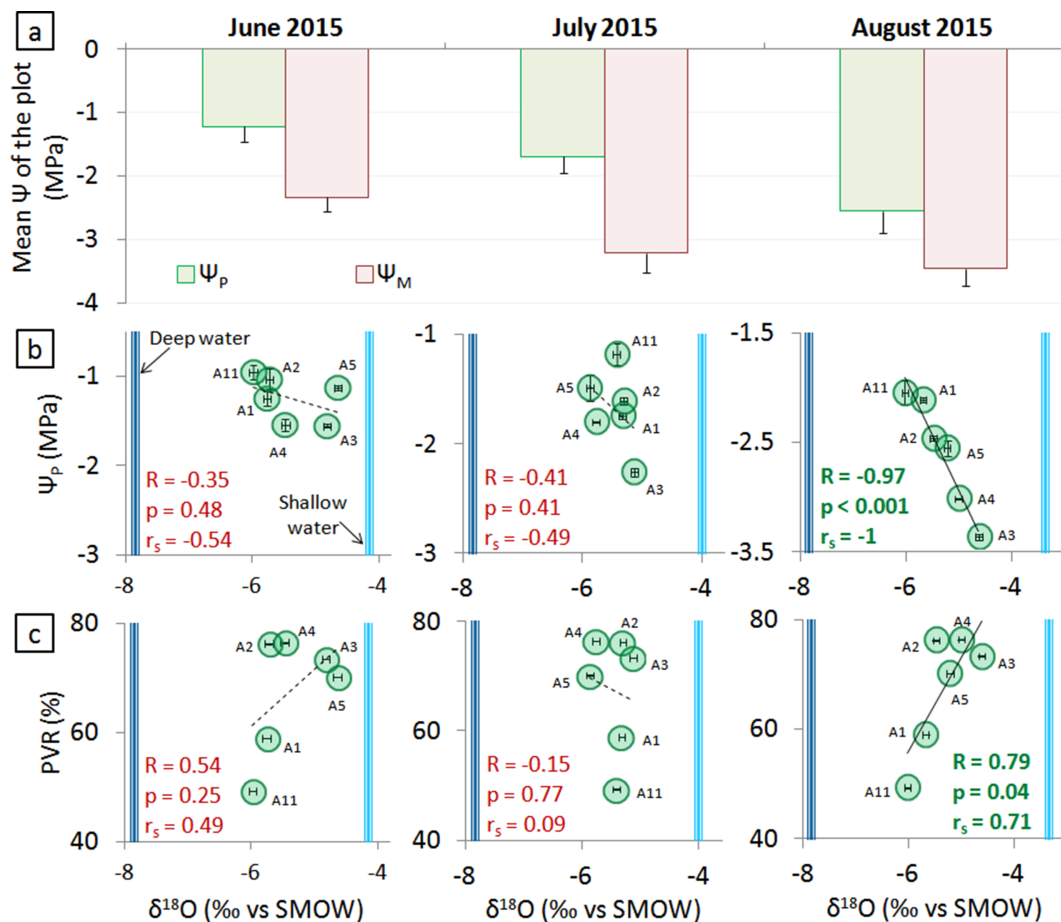


Fig. 2. a) Mean and standard deviation values for leaf water potential of the stand at predawn (Ψ_p) and midday (Ψ_M) for the months of June, July, and August 2015; b) Relationship between Ψ_p and the xylem isotope signal ($\delta^{18}O$) for each individual (each point is a tree), the dark blue and light blue vertical bars represent the groundwater and shallow water isotope signals, respectively. R is Pearson correlation, p is p-value, and r_s is Spearman correlation; c) Relationship between PVR and xylem $\delta^{18}O$ during the summer 2015.

sampled and immediately placed in a plastic bag saturated with water vapor and stored in a portable cooler until measurement (few minutes later). Between two and four leaves were measured to check the consistency between measurements. These multiple measurements were used to determine the error bars shown in Fig. 2 b and c. In the results we divided our interpretation into two periods: moderate stress ($\Psi_p > -2$ MPa) and severe stress ($\Psi_p < -2$ MPa) following the work of Lempereur et al. (2015).

2.5. Data analysis

We assumed that the isotopic dataset (Carrière et al., 2020c) is affected by an isotopic fractionation in 2H (D-fractionation), therefore we use here only ^{18}O data. D-fractionation is visible in many works (e.g. Brooks et al., 2010; Evaristo et al., 2016, 2017; Bowling et al., 2017; Geris et al., 2017; Vargas et al., 2017). The causes of this fractionation are still poorly understood (Barbeta et al., 2019). Early studies have assumed that D-fractionation is related to the mode of water absorption by roots (Sternberg and Swart, 1987; Lin and Sternberg, 1993; Ellsworth and Williams, 2007). Barbeta et al. (2020) suggest that D-fractionation is rather related to the heterogeneity of the water signal in soil pores and plant tissues. Ellsworth and Williams (2007) and Barbeta et al. (2020) agree that fractionation is much stronger in 2H than in ^{18}O and that ^{18}O provides more satisfactory analysis.

Therefore, considering only one valid tracer (^{18}O), we had to simplify our analysis into only two potential pools of plant supply: i) the shallow pool or ii) the deep pool (Fig. S12). Rain and drainage water

were analyzed separately, but the two datasets are similar during summer. We arithmetically averaged the two values to represent the “shallow water” signal in Fig. 2b and c. Deep water was collected at two seepage points (named “Point C” and “Point D”) within the LSBB tunnel (<http://lsbb.eu/presentation/>) under the experimental site. These two points were arithmetically averaged to represent the “deep water” signal of the karst vadose zone in Fig. 2b and c. We assume that this “deep water” signal corresponds to water contained within rock, as described by Bowling et al. (2017) and Geris et al. (2017).

The analysis presented in this paper is based on two previously published dataset (Carrière et al., 2020a, 2020b). Combining both datasets, only six trees were prospected by geophysics and were monitored in $\delta^{18}O$ and Ψ along the summer period 2015. The logistical difficulty for data acquisition explains this small sample. We therefore evaluated the correlation between the parameters using the Pearson correlation, but also the Spearman correlation which is recommended for the analysis of small samples.

3. Results and interpretation

3.1. Spatial variability in soil/subsoil properties at tree scale assessed with ERT

We observed wide variations in resistivity both within and between the driest and wettest profiles measured in 2011 (Fig. 1a), from $< 300 \Omega.m$ in wet conditions to $> 2500 \Omega.m$ in dry conditions. We note that the resistivity signal was more stable between the two profiles in

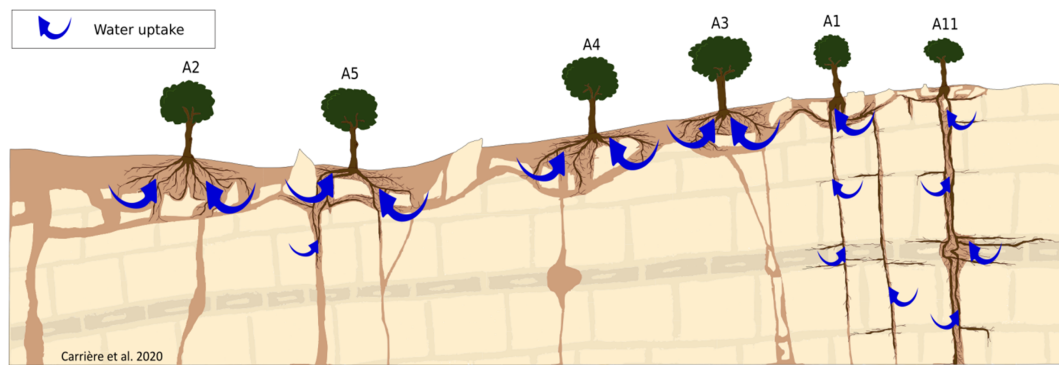


Fig. 3. Schematic interpretation of tree root implantation as a function of their soil/subsoil condition identified by geophysics (Fig. 1b), and their response to drought (Ψ_p and $\delta^{18}\text{O}$). The representation of the crown size of each tree is proportional to its individual leaf area, which is also related to soil/subsoil conditions (Carrière et al. 2020a).

deep (> 2 m) than in shallow (< 2m) layers (Fig. 1a), which caused PVR to be smaller in deeper layers (Fig. 1b).

PVR patterns showed consistent signals with field soil observations and total available water (TAW) measurements. For instance, the cross section reveals a low PVR to the right of tree A11, which is consistent with field observations showing limestone rock outcrops in this area (see SI3). We also observed a consistent trend between PVR and TAW estimated through pedologic pits (see SI4). This was discussed in Carrière et al. (2020a) and provides further evidence that PVR is well suited to quantifying TAW relatively.

In the following, PVR (0–2 m) is used as a proxy for TAW. As an example, PVR values indicate that tree A4 has a higher TAW than A11. We will examine in the following results whether these trees have contrasting $\delta^{18}\text{O}$ and Ψ_M signals. Note that the PVR is a constant value for each tree, unlike $\delta^{18}\text{O}$ and Ψ_M , which vary throughout the season.

3.2. Individual drought adaptation strategies

Tree water deficits increased during the 2015 summer season, as shown by the clear decrease in average Ψ_p and Ψ_M leaf water potentials from June to August 2015 (Fig. 2a). Concurrently, the difference between Ψ_p and Ψ_M tended to decrease during the summer season, suggesting that trees regulate their transpiration as drought increases. At the individual scale (Fig. 2b), we observed that tree A11 was systematically less stressed than tree A4. Moreover, the range of Ψ_p among individuals increased with drought.

During moderate water deficit ($\Psi_p > -2$ MPa, June and July), there was no clear relationship between Ψ_p and $\delta^{18}\text{O}$ of the xylem (Fig. 2b; p-value > 0.4). By contrast, at the peak of the drought (August 2015), we observed a significant negative relationship between Ψ_p and $\delta^{18}\text{O}$ of the xylem (p-value < 0.001). This implies that the least stressed trees (with the highest water potentials) had an isotopic signal closer to the isotopic signal of groundwater while the more stressed trees (with the lowest water potential) had an isotopic signal closer to shallow water. There was no relationship between Ψ_M and $\delta^{18}\text{O}$ at any period in 2015 (Fig. SI5). This is probably due to the fact that Ψ_M is dependent on soil water status but also on additional environmental (light and vapor pressure deficit) and biological factors (including plant hydraulic conductance, tree transpiration) that blurred its relations with soil related metrics.

Similarly, no significant relationship was observed between the isotopic signal and PVR among individuals when stress is moderate, but a significant relationship (p-value < 0.05) was observed in drier conditions (Fig. 2c). Trees with a low PVR between 0 and 2 m (i.e. low TAW) had a $\delta^{18}\text{O}$ signal closer to groundwater while trees with a high PVR (0–2 m) had an isotopic signal closer to shallow water.

4. Discussion and perspectives

The variability in drought response at the intra-specific level within a stand can be a key feature of stand resilience to climate change (Albert et al., 2012). However, the belowground processes involved in such variability remain poorly known. In Carrière et al. (2020a) we showed that trees with low near surface TAW (low PVR) experienced higher stomatal control and lower water stress during drought peak compared to trees with higher TAW, which experienced higher water stress and a higher defoliation rates following extreme drought (see SI6). In this study, for the first time, we analyzed together ERT, water potential measurements, and isotopic data to further show that there is a link between near-surface TAW, water status, and tree ability to exploit deep water.

We found a negative correlation between tree $\delta^{18}\text{O}$ and Ψ_p of individuals at the drought peak in August 2015, indicating that the individuals experiencing higher water stress relied proportionately less on deep water sources than the others. This drought dependence of the xylem isotope signal had already been demonstrated across different species (Flanagan et al., 1992; Jackson et al., 1995; Brum et al., 2019) or in the course of drought for a single species (Barbeta et al., 2015; Carrière et al., 2020b). However, to our knowledge, this is the first time that such mechanism is reported at the intra-specific level. Furthermore, we show that trees with low TAW (0–2 m) rely proportionally more on deep water during drought peaks. A likely explanation for this pattern is that trees with low TAW would have developed deeper root into the karst vadoze zone on which they could rely when drought becomes critical (Fig. 3). This hypothesis would explain why we observed an isotopic signal closer to deep water and a lower vulnerability to intense droughts for trees with higher TAW. A schematic interpretation of our results is presented in Fig. 3.

Drought resistance variability among individuals of the same species is rarely considered in ecological studies despite its role in forest structure and outcomes under ongoing climate change. Here we show strong variability between individuals that can be partially explained by underground factors (TAW, ability of trees to extract deep water). This implies that stand resistance to drought may be more heterogeneous than is currently predicted by current ecosystem models. For instance, our conclusions may explain the results of several studies showing that tree dieback following drought occurs more frequently in areas where trees benefit from well-developed soils (Nourtier et al., 2014; Preisler et al., 2019; Carrière et al., 2020a).

Further experiments should be carried out on a larger scale and on multiple species to generalize our results, and to evaluate if inter and intra-specific differences overlap. We already obtained encouraging results by enriching the Ψ_p and $\delta^{18}\text{O}$ relationship (Fig. 2b) with data observed in August 2015 on beech and silver fir trees at a nearby site located at slightly higher altitude (Fig. SI7). It would also be interesting

to assess if deep water extraction scale with root biomass in factures, that can be estimated with non-invasive method (Mary et al., 2019).

5. Conclusions

The combination of geophysics, isotopes, and foliar water potentials open fruitful research avenues to clarify plant-water relationships and tree response to drought. Significant differences in water stress were observed between the trees of the same species growing on a Mediterranean karst. Our analysis clearly suggest that such differences are due to karst heterogeneity, which imposes contrasted soil/subsoil conditions (i.e. TAW) between individual. We have shown that trees with the least favorable near-surface (0–2 m) soil/subsoil conditions proportionately extract more deep water in periods of severe stress. We hypothesize that deep water extraction can be considered as an adaptation mechanism to recurrent water deficit. It is crucial to better understand these adaptation mechanisms in order to better anticipate the impact of changes in vegetation cover on hydrological processes.

Declaration of Competing Interest

The authors declare that they have no known competing financial interests or personal relationships that could have appeared to influence the work reported in this paper.

Acknowledgments

This work benefited from fruitful discussions within the KARST observatory network (SNO KARST) initiative from the INSU/CNRS and OZCAR, which aims to strengthen knowledge sharing and promote cross-disciplinary research on karst systems at the national scale. We acknowledge H+ network of hydrogeological research sites for co-funding a part of this research. INRA supported this research in the framework of the metaprogramme Adaptation of Agriculture and Forests to Climate Change (ACCAF) of the French National Institute for Agricultural Research (INRA).

Appendix A. Supplementary data

Supplementary data to this article can be found online at <https://doi.org/10.1016/j.jhydrol.2020.125428>.

References

- Albert, C.H., de Bello, F., Boulangeat, I., Pellet, G., Lavorel, S., Thuiller, W., 2012. On the importance of intraspecific variability for the quantification of functional diversity. *Oikos* 121, 116–126.
- Allen, C.D., Macalady, A.K., Chenchouni, H., Bachelet, D., McDowell, N., Vennetier, M., Kitzberger, T., Rigling, A., Breshears, D.D., Hogg, E.T., 2010. A global overview of drought and heat-induced tree mortality reveals emerging climate change risks for forests. *For. Ecol. Manage.* 259, 660–684.
- Anderegg, W.R.L., 2015. Spatial and temporal variation in plant hydraulic traits and their relevance for climate change impacts on vegetation. *New Phytol.* 205, 1008–1014. <https://doi.org/10.1111/nph.12907>.
- Barbeta, A., Gimeno, T.E., Clavé, L., Fréjaville, B., Jones, S.P., Delvigne, C., Wingate, L., Ogée, J., 2020. An explanation for the isotopic offset between soil and stem water in a temperate tree species. *New Phytol.*
- Barbeta, A., Jones, S.P., Clavé, L., Wingate, L., Gimeno, T.E., Fréjaville, B., Wohl, S., Ogée, J., 2019. Unexplained hydrogen isotope offsets complicate the identification and quantification of tree water sources in a riparian forest. *Hydrol. Earth Syst. Sci.* 23, 2129–2146. <https://doi.org/10.5194/hess-23-2129-2019>.
- Barbeta, A., Mejía-Chang, M., Ogaya, R., Voltas, J., Dawson, T.E., Peñuelas, J., 2015. The combined effects of a long-term experimental drought and an extreme drought on the use of plant-water sources in a Mediterranean forest. *Glob. Change Biol.* 21, 1213–1225. <https://doi.org/10.1111/gcb.12785>.
- Bonan, G.B., 2008. Forests and climate change: forcings, feedbacks, and the climate benefits of forests. *Science* 320, 1444–1449.
- Bontemps, A., Davi, H., Lefèvre, F., Rozenberg, P., Oddou-Muratario, S., 2017. How do functional traits syndromes covary with growth and reproductive performance in a water-stressed population of *Fagus sylvatica*? *Oikos* 126, 1472–1483.
- Bowling, D.R., Schulze, E.S., Hall, S.J., 2017. Revisiting streamside trees that do not use stream water: can the two water worlds hypothesis and snowpack isotopic effects explain a missing water source? *Ecohydrology* 10, e1771.
- Brooks, J.R., Barnard, H.R., Coulombe, R., McDonnell, J.J., 2010. Ecohydrologic separation of water between trees and streams in a Mediterranean climate. *Nat. Geosci.* 3, 100.
- Brum, M., Vadeboncoeur, M.A., Ivanov, V., Asbjornsen, H., Saleska, S., Alves, L.F., Penha, D., Dias, J.D., Aragão, L.E., Barros, F., 2019. Hydrological niche segregation defines forest structure and drought tolerance strategies in a seasonal Amazon forest. *J. Ecol.* 107, 318–333.
- Carrière, S.D., Ruffault, J., Pimont, F., Doussan, C., Simioni, G., Chalikakis, K., Limousin, J.-M., Scotti, I., Courdier, F., Cakpo, C.-B., 2020a. Impact of local soil and subsoil conditions on inter-individual variations in tree responses to drought: insights from Electrical Resistivity Tomography. *Sci. Total Environ.* 698, 134247.
- Carrière, S.D., Martin-StPaul, N.K., Cakpo, C.B., Patris, N., Gillon, M., Chalikakis, K., Doussan, C., Oliosio, A., Babic, M., Jouineau, A., Simioni, G., Davi, H., 2020b. The role of deep vadose zone water in tree transpiration during drought periods in karst settings—Insights from isotopic tracing and leaf water potential. *Sci. Total Environ.* 699, 134332.
- Carrière, S.D., Martin-StPaul, N.K., Cakpo, C.B., Patris, N., Gillon, M., Chalikakis, K., Doussan, C., Oliosio, A., Babic, M., Jouineau, A., 2020c. Tree xylem water isotope analysis by Isotope Ratio Mass Spectrometry and Laser Spectrometry: a dataset to explore tree response to drought. *Data in Brief* 105349.
- Carrière, S.D., Danquigny, C., Davi, H., Chalikakis, K., Ollivier, C., Martin-StPaul, N.K., Emblanch, C., 2017. Process-based vegetation models improve karst recharge simulation under Mediterranean forest. In: *EuroKarst 2016*, Neuchâtel. Springer, pp. 109–116.
- Carrière, S.D., Chalikakis, K., Danquigny, C., Davi, H., Mazzilli, N., Ollivier, C., Emblanch, C., 2016. The role of porous matrix in water flow regulation within a karst unsaturated zone: an integrated hydrogeophysical approach. *Hydrogeol. J.* 24, 1905–1918.
- Carrière, S.D., Chalikakis, K., Danquigny, C., Clément, R., Emblanch, C., 2015. Feasibility and limits of electrical resistivity tomography to monitor water infiltration through karst medium during a rainy event. In: *Andreo, B., Carrasco, F., Durán, J.J., Jiménez, P., LaMoreaux, J.W. (Eds.), Hydrogeological and Environmental Investigations in Karst Systems*. Springer, Berlin Heidelberg, pp. 45–55. https://doi.org/10.1007/978-3-642-17435-3_6.
- Carrière, S.D., Chalikakis, K., Sénéchal, G., Danquigny, C., Emblanch, C., 2013. Combining electrical resistivity tomography and ground penetrating radar to study geological structuring of karst unsaturated zone. *J. Appl. Geophys.* 94, 31–41. <https://doi.org/10.1016/j.jappgeo.2013.03.014>.
- Chalikakis, K., Plagnes, V., Guerin, R., Valois, R., Bosch, F.P., 2011. Contribution of geophysical methods to karst-system exploration: an overview. *Hydrogeol. J.* 19, 1169–1180. <https://doi.org/10.1007/s10040-011-0746-x>.
- Clément, R., Desclotres, M., Günther, T., Oxarango, L., Morra, C., Laurent, J.P., Gourc, J.P., 2010. Improvement of electrical resistivity tomography for leachate injection monitoring. *Waste Manage.* 30, 452–464. <https://doi.org/10.1016/j.wasman.2009.10.002>.
- Dahlin, T., 2001. The development of DC resistivity imaging techniques. *Comput. Geosci.* 27, 1019–1029. [https://doi.org/10.1016/S0098-3004\(00\)00160-6](https://doi.org/10.1016/S0098-3004(00)00160-6).
- Dawson, T.E., 1993. Hydraulic lift and water use by plants: implications for water balance, performance and plant-plant interactions. *Oecologia* 95, 565–574.
- Ding, Y., Nie, Y., Schwinning, S., Chen, H., Yang, J., Zhang, W., Wang, K., 2018. A novel approach for estimating groundwater use by plants in rock-dominated habitats. *J. Hydrol.* 565, 760–769.
- Ehleringer, J., Dawson, T., 1992. Water uptake by plants: perspectives from stable isotope composition. *Plant Cell Environ.* 15, 1073–1082.
- Ellsworth, P.Z., Williams, D.G., 2007. Hydrogen isotope fractionation during water uptake by woody xerophytes. *Plant Soil* 291, 93–107.
- Evaristo, J., McDonnell, J.J., Clemens, J., 2017. Plant source water apportionment using stable isotopes: a comparison of simple linear, two-compartment mixing model approaches. *Hydrol. Process.* 31, 3750–3758. <https://doi.org/10.1002/hyp.11233>.
- Evaristo, J., McDonnell, J.J., Scholl, M.A., Bruijnzeel, L.A., Chun, K.P., 2016. Insights into plant water uptake from xylem-water isotope measurements in two tropical catchments with contrasting moisture conditions. *Hydrol. Process.* 30, 3210–3227.
- Fisher, J.B., Melton, F., Middleton, E., Hain, C., Anderson, M., Allen, R., McCabe, M.F., Hook, S., Baldocchi, D., Townsend, P.A., 2017. The future of evapotranspiration: Global requirements for ecosystem functioning, carbon and climate feedbacks, agricultural management, and water resources. *Water Resour. Res.* 53, 2618–2626.
- Flanagan, L., Ehleringer, J., Marshall, J., 1992. Differential uptake of summer precipitation among co-occurring trees and shrubs in a pinyon-juniper woodland. *Plant Cell Environ.* 15, 831–836.
- Geris, J., Tetzlaff, D., McDonnell, J.J., Soulsby, C., 2017. Spatial and temporal patterns of soil water storage and vegetation water use in humid northern catchments. *Sci. Total Environ.* 595, 486–493.
- Hartmann, A., Goldscheider, N., Wagoner, T., Lange, J., Weiler, M., 2014. Karst water resources in a changing world: review of hydrological modeling approaches. *Rev. Geophys.* 52, 218–242. <https://doi.org/10.1002/2013RG000443>.
- IAEA, 2014. IAEA/GNIP precipitation sampling guide [WWW Document]. accessed 1.23.19. http://www-naweb.iaea.org/napc/ih/documents/other/gnip_manual_v2_02_en_hq.pdf.
- Jackson, P., Cavelier, J., Goldstein, G., Meinzer, F., Holbrook, N., 1995. Partitioning of water resources among plants of a lowland tropical forest. *Oecologia* 101, 197–203.
- Jourde, H., Massei, N., Binet, S., Batiot-Guilhe, C., Labat, D., Steinmann, M., Bailly-Comte, V., Seidel, J., Arfib, B., 2018. SNO KARST: A French network of observatories for the multidisciplinary study of critical zone processes in karst watersheds and aquifers. *Vadose Zone J.* 17.
- Keller, G.V., Frischknecht, F.C., 1966. Electrical methods in geophysical prospecting.

- International Series of Monographs in Electromagnetic Waves 10.
- Kirilenko, A.P., Sedjo, R.A., 2007. Climate change impacts on forestry. *Proc. Natl. Acad. Sci.* 104, 19697–19702.
- Lempereur, M., Martin-StPaul, N.K., Damesin, C., Joffre, R., Ourcival, J., Rocheteau, A., Rambal, S., 2015. Growth duration is a better predictor of stem increment than carbon supply in a Mediterranean oak forest: implications for assessing forest productivity under climate change. *New Phytol.* 207, 579–590.
- Lin, G., da Sternberg, L.S.L., 1993. Hydrogen isotopic fractionation by plant roots during water uptake in coastal wetland plants. In: *Stable Isotopes and Plant Carbon-Water Relations*. Elsevier, pp. 497–510.
- Love, D., Venturas, M., Sperry, J., Brooks, P., Pettit, J.L., Wang, Y., Anderegg, W., Tai, X., Mackay, D., 2019. Dependence of aspen stands on a subsurface water subsidy: Implications for climate change impacts. *Water Resour. Res.* 55, 1833–1848.
- Maréchal, J.-C., Varma, M.R., Riotte, J., Vouillamoz, J.-M., Kumar, M.M., Ruiz, L., Sekhar, M., Braun, J.-J., 2009. Indirect and direct recharges in a tropical forested watershed: mule hole, India. *J. Hydrol.* 364, 272–284.
- Martín-Gómez, P., Barbeta, A., Voltas, J., Peñuelas, J., Dennis, K., Palacio, S., Dawson, T.E., Ferrio, J.P., 2015. Isotope-ratio infrared spectroscopy: a reliable tool for the investigation of plant-water sources? *New Phytol.* 207, 914–927.
- Mary, B., Vanella, D., Consoli, S., Cassiani, G., 2019. Assessing the extent of citrus trees root apparatus under deficit irrigation via multi-method geo-electrical imaging. *Sci. Rep.* 9, 9913.
- Mathys, A., Coops, N.C., Waring, R.H., 2014. Soil water availability effects on the distribution of 20 tree species in western North America. *For. Ecol. Manage.* 313, 144–152.
- Nie, Y., Chen, H., Wang, K., Yang, J., 2012. Water source utilization by woody plants growing on dolomite outcrops and nearby soils during dry seasons in karst region of Southwest China. *J. Hydrol.* 420, 264–274.
- Nourtiert, M., Chanzy, A., Cailleret, M., Yingge, X., Huc, R., Davi, H., 2014. Transpiration of silver Fir (*Abies alba* mill.) during and after drought in relation to soil properties in a Mediterranean mountain area. *Ann. For. Sci.* 71, 683–695.
- Nosetto, M.D., Jobbágy, E., Brizuela, A.B., Jackson, R., 2012. The hydrologic consequences of land cover change in central Argentina. *Agric. Ecosyst. Environ.* 154, 2–11.
- Oki, T., Kanae, S., 2006. Global hydrological cycles and world water resources. *Science* 313, 1068–1072.
- Preisler, Y., Tatarinov, F., Grünzweig, J.M., Bert, D., Ogée, J., Wingate, L., Rotenberg, E., Rohatyn, S., Her, N., Moshe, I., 2019. Mortality versus survival in drought-affected Aleppo pine forest depends on the extent of rock cover and soil stoniness. *Funct. Ecol.* 33, 901–912.
- Pivovarov, A.L., Pasquini, S.C., De Guzman, M.E., Alstad, K.P., Stemke, J.S., Santiago, L.S., 2016. Multiple strategies for drought survival among woody plant species. *Funct. Ecol.* 30, 517–526. <https://doi.org/10.1111/1365-2435.12518>.
- Querejeta, J.I., Estrada-Medina, H., Allen, M.F., Jiménez-Osornio, J.J., 2007. Water source partitioning among trees growing on shallow karst soils in a seasonally dry tropical climate. *Oecologia* 152, 26–36.
- Rambal, S., Ourcival, J.-M., Joffre, R., Mouillot, F., Nouvellon, Y., Reichstein, M., Rocheteau, A., 2003. Drought controls over conductance and assimilation of a Mediterranean evergreen ecosystem: scaling from leaf to canopy. *Glob. Change Biol.* 9, 1813–1824. <https://doi.org/10.1111/j.1365-2486.2003.00687.x>.
- Robert, T., Caterina, D., Deceuster, J., Kaufmann, O., Nguyen, F., 2012. A salt tracer test monitored with surface ERT to detect preferential flow and transport paths in fractured/karstified limestones. *Geophysics* 77, B55–B67. <https://doi.org/10.1190/geo2011-0313.1>.
- Scanlon, B.R., Reedy, R.C., Stonestrom, D.A., Prudic, D.E., Dennehy, K.F., 2005. Impact of land use and land cover change on groundwater recharge and quality in the southwestern US. *Glob. Change Biol.* 11, 1577–1593. <https://doi.org/10.1111/j.1365-2486.2005.01026.x>.
- Sternberg, L. da S.L., Swart, P.K., 1987. Utilization of freshwater and ocean water by coastal plants of southern Florida. *Ecology* 68, 1898–1905.
- Taylor, R.G., Scanlon, B., Doll, P., Rodell, M., van Beek, R., Wada, Y., Longuevergne, L., Leblanc, M., Famiglietti, J.S., Edmunds, M., Konikow, L., Green, T.R., Chen, J., Taniguchi, M., Bierkens, M.F.P., MacDonald, A., Fan, Y., Maxwell, R.M., Yechieli, Y., Gurdak, J.J., Allen, D.M., Shamsudduha, M., Hiscock, K., Yeh, P.J.F., Holman, I., Treidel, H., 2013. Ground water and climate change. *Nature Clim. Change* 3, 322–329. <https://doi.org/10.1038/nclimate1744>.
- Turner, N.C., 1981. Techniques and experimental approaches for the measurement of plant water status. *Plant Soil* 58, 339–366.
- Vargas, A.I., Schaffer, B., Yuhong, L., da Sternberg, L., S.L., 2017. Testing plant use of mobile vs immobile soil water sources using stable isotope experiments. *New Phytol.* 215, 582–594.
- Voltas, J., Lucabaugh, D., Chambel, M.R., Ferrio, J.P., 2015. Intraspecific variation in the use of water sources by the circum-Mediterranean conifer *Pinus halepensis*. *New Phytol.* <https://doi.org/10.1111/nph.13569>.
- West, A.G., Patrickson, S.J., Ehleringer, J.R., 2006. Water extraction times for plant and soil materials used in stable isotope analysis. *Rapid Commun. Mass Spectrom.* 20, 1317–1321. <https://doi.org/10.1002/rcm.2456>.